

# Domain Adversarial Learning Towards Underwater Image Enhancement

Meghna Kapoor, Rohan Baghel, Badri Narayan Subudhi, Vinit Jakhetiya, Ankur Bansal  
Indian Institute of Technology Jammu  
Jammu and Kashmir, India

{meghna, 2021PCS1025, subudhi.badri, vinit.jakhetiya, ankur.bansal}@iitjammu.ac.in

## Abstract

*Underwater images are degraded due to the absorption and scattering of light inside the water. The underwater degradation causes the loss of information in terms of texture, style, color, and minute detail of edges and hence the degraded images are not useful in many higher-order applications. Several deep learning techniques are explored by researchers across the globe for the same. Further, deep learning networks learn the distribution of degraded training samples and fail when there is a deviation due to a change in water type. This paper proposes an encoder-decoder network that preserves the image content, texture, and style while maintaining overall global similarity by capturing the inherent distribution of the training samples. To overcome the deviation due to a change in water type, a classifier network is induced in the latent space of encoder-decoder architecture. The classifier loss and adversarial loss in the classifier network ensure the learning across domains and avoid setting priors on captured distribution. Hence, the proposed model is robust against the change of water type and can be deployed in real-life without re-training. To train the model, we use attenuation coefficients of underwater environments at different depths to recreate 5430 paired underwater images from the Underwater Image Enhancement Benchmark (UIEB) dataset with six distinct types of water. Our proposed model enhanced the degraded images among different degradation levels due to depth and water type variations. The proposed model is evaluated on UIEB and EUVP benchmark databases. The performance of the proposed model is verified against twenty-two state-of-the-art methods in terms of underwater reference and no-reference image quality assessment metrics.*

## 1. Introduction

In the last few years, underwater surveillance has gained a lot of attention due to various applications including, underwater object tracking [1], underwater pipeline fault detection [2], autonomous underwater vehicle navigation [3],

etc. It is observed that most underwater surveillance techniques are highly affected by poor-quality underwater images. Underwater images are distorted in terms of color, brightness, and contrast due to suspended particles and underwater intrinsic properties while the light travel inside the water. The reflected light travels from the object to the camera in water, suffering from two phenomena: absorption and scattering. Jaffe-McGlamery [4] models the total light perceived by the camera as the sum of the three components: direct, forward-scattered, and backward-scattered.

The state-of-the-art techniques focus on restoring the clearer image by altering the contrast and brightness levels based on histogram-based methods [5, 6, 7, 6] or channel-based priors-based methods [8, 9, 10]. However, such methods are not reliable in real-life scenarios and fail to characterize the scene complexities due to underwater dynamics. Recently, deep learning-based techniques [11, 12, 13] are gaining popularity due to their inherent capabilities of extracting deep features and compensating for the level of degradation to produce an enhanced image. However, these methods rely heavily on the training set distribution to assess the level of degradation and produce an enhanced image. Again, the water condition is not the same at every place due to the change in temperature, weather, viscosity, etc. Further, around the coast, the water is muddy, and in the oceanic environment presence of saline water changes the refractive index of the medium and hence the level of degradation. The deviation in environmental conditions and change in water type leads to a distribution shift between the training and the testing sets. Hence, the state-of-the-art (SOTA) methods cannot address the underwater dynamics and the variation in degradation levels based on different water types.

In this paper, we attempt to address the challenge of underwater dynamics by designing an adversarial learning-based end-to-end encoder-decoder architecture to enhance the underwater images. We proposed the reconstruction loss for preserving the video scene's minute details in encoder-decoder architecture to produce an enhanced image. Reconstruction loss enhances the image by maintaining global

similarity and considering the content of the image. Also preserves the overall style and texture. However, it has been observed the decoder devises a prior water type based on the features extracted by the encoder and enhances the image accordingly. Hence, different levels of degradation in image frames when they are captured at varied depths and water types are not considered using encoder-decoder architectures. To mitigate this issue, we proposed a CNN-based classifier network in latent space. The intuition behind designing the classifier is to deploy the domain adversarial learning by capturing the distribution of video scenes using classifier focal loss and adversarial loss. During the training, the encoder-decoder model is not converged entirely to incorporate the change in water type using a classifier convolutional network. When the encoder-decoder model reaches a pre-decided threshold, the classifier network is introduced at latent space to make the model agnostic to handle the variation in water type. Hence, the proposed model does not require re-training to capture the variation in the scene and uses domain adversarial learning to produce enhanced images. The number of classes in the training set depicting different types of water need not be the same. Hence, we propose to use focal loss on the classifier network to avoid setting any prior on a specific class. The shift in distribution is captured by adversarial loss to obtain an enhanced image without any assumption of the amount of degradation in the input image.

Further, the state-of-the-art underwater image datasets are not capable to characterize different water types and hence are unable to model different distributions. We proposed a strategy to recreate a new synthetic underwater dataset derived from the Underwater Image Enhancement Benchmark (UIEB) dataset [14] with different attenuation levels and varied depths. The dataset has been expanded to 5340 images, representing six distinct types of water.

The main contribution of this paper are listed below;

- We proposed adversarial learning of the underwater image domain, resulting in improved visually enhanced underwater images across different levels of degradation across varied attenuation levels and depth.
- The proposed architecture induces a focal loss in the classifier to label the correct water type based on extracted features in the latent space.
- We proposed to induce adversarial loss on the classifier to generalize a pre-trained model and capture the deviation in distribution due to variation in water type.
- We introduce the recreation of a new synthetic underwater dataset derived from the Underwater Image Enhancement Benchmark (UIEB) dataset [14], consisting of 890 underwater reference images. The dataset has

been expanded to 5340 images, representing six distinct types of water.

The rest of the paper is organized as follows. Section 2 depicts the state-of-the-art techniques in underwater image enhancement. The proposed method is provided in detail in Section 3. Section 4 contains the model to create the synthetic dataset. The experimental setup along with the visual and quantitative analysis of results are discussed in Section 5. Finally, Section 6 concludes the proposed work along with discussions regarding the future scope of the work.

## 2. Related Work

Enhancing the quality of the underwater images is one of the essential tasks for improving the interpretability and increasing the overall information of the captured scene. The state-of-the-art technique for underwater image enhancement can be divided into two sub-categories: conventional and deep learning-based.

### 2.1. Conventional methods

The conventional methods aim to enhance the image to bring out the obscured details from the underwater images by altering the distribution of intensities or stretching the contrast by pixel level transform to get an enhanced image. The methods like color correction, contrast enhancement, color prior, and noise reduction techniques are applied to the degraded image to get an enhanced image. The conventional underwater image enhancement methods can be categorized into two sub-categories: contrast enhancement and channel prior.

#### 2.1.1 Contrast Enhancement based Techniques

The contrast enhancement schemes use the application of single-valued and monotonically increasing functions in mapping the pixel level or spatial domain processing for improving the contrast of an image. In a high-contrast image, the variation of pixel intensities belonging to foreground or background is quite significant resulting in the preservation of information. Agalan *et al.* [5] proposed a method of contrast enhancement based on the properties of logarithmic transform coefficient histograms. The said method applies the transformation map in terms of logarithmic scale to the original image. The lower intensities are expanded, and higher intensities are compressed. Further, researchers in [15, 16] relied on logarithmic transform histogram matching to obtain an enhanced image. However, these methods fail to address the loss of color information in the local regions of an image. Further, the contrast enhancement factor is used to adjust the pixel values, improving the color and contrast of the image. The histogram equalization methods

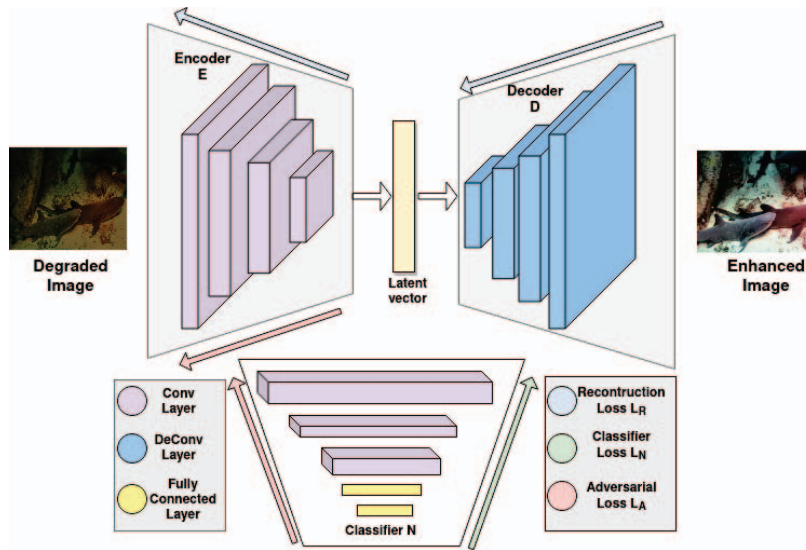


Figure 1: Architecture of proposed model. The left-hand side is the encoder part and the right-hand side is the decoder part. A classifier is built to generalize the loss depicted in the bottom part between the encoder and decoder.

[6, 17] help in contrast adjustment, yet they fail to incorporate the surrounding dynamics.

### 2.1.2 Channel Prior based Techniques

Channel prior techniques aim to assess the degradation of underwater images and enhance their quality based on pre-defined priors set on intensity distribution theories. One such theory is dark channel prior which assumes at least one channel has a very low intensity for a haze-free image. Methods like [8, 9, 18, 19, 20, 9] focus on using the dark channel prior for enhancing the underwater images. However, the distortion happens most across the red channel, so setting a prior on the red channel is a more obvious choice. Researchers [21, 22, 23, 24] focused on enhancing the underwater images assuming the red channel must have the lowest intensity. The variational models enhance the image by estimating reflectance and illumination in a retinex decomposition. The authors in [10, 25, 26] used hyper-Laplacian reflectance priors to increase the quality of the image. However, it is observed that, in real-life scenarios, setting a prior is not always feasible. Recently, deep learning methods have performed better in underwater image enhancement as they learn the distribution of the underwater dynamism at a deeper level to retrieve an enhanced image.

## 2.2. Deep learning-based methods

Deep learning-based methods for enhancing underwater images primarily rely on deep convolutional neural networks based deep features analysis to improve the image quality. These techniques use large datasets of underwater images to train the network to learn the underlying pat-

terns and relationships between the input and output images. Compared to conventional methods, deep learning-based methods have been shown to produce high-quality underwater images with improved contrast, brightness, and color saturation. Deep convolutional neural networks estimate the degradation among pixel intensities and retrieve an enhanced image. A lot of state-of-the-art methods [27, 28, 23] focus on deep convolutional network-based image enhancement techniques to bring out the obscured details from the degraded images. One such work was reported by Wang *et al.* [29], where the CNN-based color correction scheme for underwater images is proposed. Recently, generative adversarial networks gained popularity due to their ability to produce an enhanced image based on the distribution of target classes. Methods like [30, 31, 32, 33, 34] use GAN to enhance the degraded underwater images. Chen *et al.* [11] propose a twin adversarial contrastive learning-based underwater image enhancement model. However, it may be observed that most of the discussed models are not deployable in real-life scenarios as they failed in the scenario where there is a significant change in the distribution of the testing set from the training set. Uplavikar *et al.* [13] proposed a method for underwater image enhancement across different domains. The method uses a synthetic indoor dataset to mimic the underwater enhancement. Hence, the said method doesn't cover underwater dynamics.

## 3. Proposed Method

In this paper, we propose an end-to-end encoder-decoder architecture for removing the degradation in underwater images. The complete architecture of the proposed model is

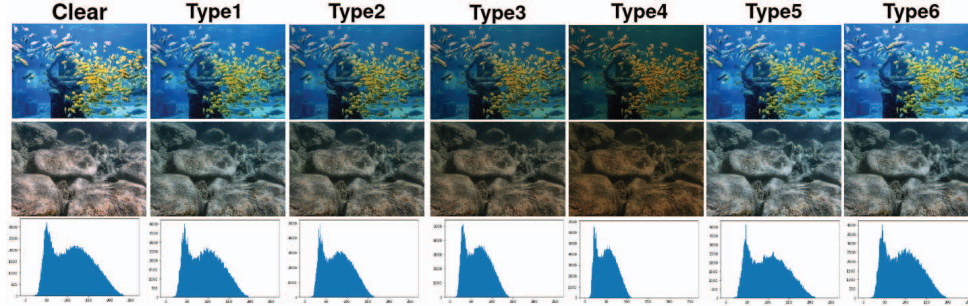


Figure 2: An example set of synthetic images from our dataset comprising six classes. First column contains the clear images and column two to seven contains degraded images regenerated using Table 1. The first and second row contains the sample images, and the third row depicts the variation in intensity distribution at different levels of degradation.

shown in Figure 1. The main idea of the proposed model is to enhance the model’s generalization ability for producing distortion-free images irrespective of the variation in the distribution of testing samples from the training samples. The model comprises an encoder ( $E$ ), a decoder ( $D$ ), and a water-type classifier ( $N$ ). The encoder-decoder network is a convolutional neural network designed to generate clear image by compensating any degradation. We introduce a classifier ( $N$ ) to classify the water type from the latent vector ( $Z$ ) projected at the end of the encoder. The objective of this endeavor is not solely to train the model and generate an improved image but rather to instill the model with an understanding of the intrinsic characteristics of underwater images. Hence, we proposed to explore the capabilities of domain adversarial learning using a combination of classifier and adversarial loss to train the encoder to be more agnostic of different water types. Adding these loss terms ensures the regularization of features represented as latent vectors ( $Z$ ) for capturing the general data distribution.

### 3.1. Proposed Network Architecture

The proposed network comprises an end-to-end architecture with the encoder-decoder network to get an enhanced image. Herewith we propose a classifier network for domain adversarial learning-induced in between the encoder-decoder network. Figure 1 represents the same.

#### 3.1.1 Encoder-Decoder Network

The input image is fed to an encoder ( $E$ ) to generate a latent vector ( $Z$ ). There are four blocks each in the encoder and the decoder part. The encoder block combines the convolution layer, batch normalization followed by ReLU to extract the features, and max pooling to down-sample the feature map. The decoder part uses bilinear up-sampling followed by convolution and batch normalization. The nonlinearity is added to the network using the ReLU activation function. The output from the last layer of the decoder is given to

a non-linear activation unit ( $\tanh$ ) to produce a distortion-free image.

#### 3.1.2 Classifier Network

We propose an induction of the classifier network in the architecture to prevent the latent space vector to have a prior about the water type based on the extracted features. The classifier network consists of the convolutional neural network followed by batch normalization and ReLU. The feature map is flattened after pooling to construct a fully connected layer. The water type is defined over the categories defined over the number of classes in the dataset.

#### 3.1.3 Domain Adversarial Learning

It may be observed in SOTA that, while the deployment of deep learning models, the system’s performance degrades due to the shift in the distribution of source and target images. In underwater imaging, this shift can be observed with the deviation in the water type or variation in underwater environment conditions from training. Hence in this work, we proposed a combination of classifier and adversarial loss together to address the said issue. The proposed encoder-decoder architecture is used to extract the features representing the source domain. In the classifier network, we proposed to induce the classifier loss to predict the water type accurately by minimizing the maximum mean divergence between the encoder and the classifier. Hence, a label can be assigned even if the distribution varies between the source and the target class. Further, we propose adversarial learning which trains the encoder to produce domain invariant features such that the source and target water type is indistinguishable by the decoder. Hence, applying domain adversarial learning with the combination of classifier and adversarial loss ensures the generalization ability of the proposed model.

### 3.2. Loss Functions

We proposed a combination of three loss functions: the reconstruction loss ( $L_R$ ), the classifier loss ( $L_N$ ), and the adversarial loss ( $L_A$ ) [35] in the proposed network. These losses are deployed to generate clearer images and to train our encoder to be more agnostic of different water types. Further, we proposed the reconstruction loss at the end of the decoder and updates the weights of both the encoder and decoder. It ensures that the generated images are clear and that important information is retained during the encoding and decoding process. During training, first the encoder-decoder model is converged using only reconstruction loss till an accuracy of 90% is achieved. Then, to make the model free from any prior on dataset, a combination of classifiers loss and adversarial loss is induced in classifier network. These two losses ensure the optimization of the classifier network and encoder. Hence, the model will be able to generate clear images while predicting the water type over a more general distribution. Classifier loss predicts the water type of the latent vector, which helps the decoder generate a clear image. This loss function is used to guide the decoder to generate images that are consistent with the water type indicated by the latent vector. Further, the distribution function of the target may deviate from the present one. To design a system free from any prior set of the extracted features in latent space, an adversarial loss is used to generate a clear image irrespective of water type. These losses are described as follows:

#### 3.2.1 Reconstruction Loss

The underwater images are blurred resulting in a reduction of local and global information. Moreover, the enhanced image obtained from the decoder loses information during projecting back from latent space to image space. Hence, we introduced the reconstruction loss in the network by considering three parameters: global similarity, image content, and local texture and style information to get an enhanced image.

- **Global similarity:** The global similarity loss function helps in enforcing a similarity between the generated output and the target consistent with the  $L1$  metric [36, 37]. Minimizing the  $L1$  loss encourages the model to produce a globally consistent output with the target image and it is less susceptible to the effects of blurriness.

$$\mathcal{L}_1 = \sum_{i=1}^N |Y - D(Z)|, \quad (1)$$

where,  $N$  is the number of pixels,  $X$  is a distorted image,  $Y$  is the ground truth image, and latent vector  $Z = E(X)$ ,  $E$  refers to the encoder and  $D$  refers to the Decoder of the model.

- **Image content:** A content loss is added to ensure that the enhanced image has similar content as the ground truth image. This loss is defined using a pre-trained convolutional neural network as in [38, 39], Image content loss is Euclidean distance between feature representations of the enhanced and target images.

$$\mathcal{L}_{con} = \frac{1}{C_j H_j W_j} \|\psi_j(D(Z)) - \psi_j(Y)\|, \quad (2)$$

where,  $\psi_j()$  is a feature map obtained from  $j^{th}$  layer of the convolutional neural network,  $C_j$ ,  $H_j$  and  $W_j$  denotes the number, height, and width of the feature map,  $X$  is the distorted image,  $Y$  is the ground truth image, and latent vector  $Z = E(X)$ ,  $E$  refers to the encoder and  $D$  refers to the Decoder of the model.

- **Local texture and style:** The mean squared error (MSE) loss is utilized to capture high-frequency information that pertains to local texture and style. This enables the encoder to generate an enhanced image while retaining texture and style. The MSE can be given as,

$$\mathcal{L}_{loc} = \frac{1}{N} \sum_{i=1}^N |D(Z)_i - Y_i|^2. \quad (3)$$

where  $N$  is the number of pixels.

The reconstruction loss is formulated to guide the generator ( $G$ ) in learning and improving the image quality such that the generated enhanced image is close to the ground truth image defined as,

$$L_R = \mathcal{L}_{loc} + \lambda_1 \mathcal{L}_1 + \lambda_c \mathcal{L}_{con}. \quad (4)$$

where  $\lambda_1$  and  $\lambda_c$  are hyper-parameters defined as 0.7 and 0.3, empirically.

#### 3.2.2 Classifier Loss

We proposed the use of classification loss in terms of a focal loss [40] to capture the distribution of type of water and is utilized to update the classifier ( $N$ ). The focal loss is widely used in object detection to address the class imbalance problem. During training, random sampling leads to creating an imbalance in the number of samples used for training from each class. A focus is given on the examples that the model is finding difficult to classify. The loss is defined as follows,

$$L_N = -(1 - p_t)^\gamma * \log(p_t). \quad (5)$$

where  $p_t$  is the probability of the classification in the correct class, and  $\gamma$  is the tunable parameter defining the focus given to a particular class.

### 3.2.3 Adversarial loss

To generate the enhanced images independent of any particular water type adversarial loss is used. The adversarial loss ( $L_A$ ) is the negative entropy of the predicted distribution of the water type produced by the classifier for the latent vector ( $Z$ ).

$$L_A(X) = \sum_{c=1}^M N(Z)_c \log N(Z)_c. \quad (6)$$

where  $Z = E(X)$ , and  $M$  is the number of classes. The latent vector  $Z$  is fed to the water-type classifier  $N$  to capture the deviation between the distribution of source and target domains.

## 4. Recreation of the Dataset

The underwater images are degraded due to the absorption and scattering of light. According to the underwater image formation model, the captured image can be expressed as shown in eq 7

$$U_\lambda(z) = I_\lambda(x) * K_\lambda(z) + B_\lambda(1 - K_\lambda(z)). \quad (7)$$

where  $U_\lambda(z)$  is the captured underwater image,  $I_\lambda(x)$  is the clear latent image,  $B_\lambda$  is the homogeneous background light, and  $K_\lambda(z)$  is the medium energy ratio. The underwater degradation level is different at varied depths and in different water types. The degradation coefficients are also not the same at different water conditions like oceanic and coastal depths. The attenuation coefficient ( $K_d(z, \lambda)$ ) depends on the energy of the light beam ( $E$ ) and is given as,

$$K_\lambda(z) = 10^{-\beta_\lambda d(z)} = -\frac{E_\lambda(z, d(z))}{E_\lambda(z, 0)}. \quad (8)$$

Here,  $\beta_\lambda$  is the medium attenuation coefficient, and distance  $d(z)$  is the distance from scene point  $z$  to the camera. The value of attenuation differs at different depths ( $z$ ) and for different wavelengths ( $\lambda$ ) [44]. The transition between attenuation coefficient  $K_\lambda$  for different channels is not straightforward and differs in all three (R, G, B) channels [45]. Addressing and retaining information across different water types becomes challenging using mathematical modeling. In this paper, we designed an encoder-decoder-based architecture to incorporate the difference in degradation in different water bodies with respect to depth. The SOTA methods capture the distribution of the training set. In real-life scenarios, the testing set distribution deviates from the training set due to various environmental conditions like changes in weather, temperature, and

lighting conditions. The domain adversarial learning handles the change in distribution without re-training the entire network. The SOTA methods require fine-tuning or re-training in order to incorporate the deviation of testing distribution from training distribution. However, most of the existing benchmark datasets are consistent as they do not have enough images from different water types. Hence, it needs a dataset that can address the scarcity of proper data required from different water types at different levels. To address the same, we propose to recreate the UIEB database with different water types.

Table 1: Classes description and attenuation coefficients of the synthetic dataset

Class in our dataset	Channel		
	red	green	blue
1	0.81	0.96	0.98
2	0.75	0.89	0.89
3	0.75	0.89	0.88
4	0.67	0.73	0.67
5	0.62	0.61	0.50
6	0.55	0.46	0.29

To recreate the synthetic dataset, we degraded the values in R, G, and B color channels of the images present in the UIEB dataset in order to create views in different water types. As the condition deviates the attenuation among the channels differs. An empirical study was performed by Jerlov [46] to study the attenuation at different depths and weather conditions. Along similar lines, we defined attenuation coefficients and defined six classes in our proposed model to recreate the EUVP dataset. The change in water type directly impacts the turbidity of the water. Classes: one to four represent oceanic water conditions and classes five and six represent the coastal water conditions.

In the proposed, underwater recreation model we have used attenuation across each type in R, G B channels of the underwater image as given in Table 1. The medium attenuation is varied between a range of  $\{0.8, 1\}$  and a depth of 0.5m to 15m is considered. These values are put in equations 7 and 8 to get channel-wise attenuation and create degraded images. Applying the degradation coefficient on the samples of the UIEB dataset, we have created a dataset comprised of six classes. The description is given in Table: 1 and the sample images are shown in Figure 2. The proposed scheme recreates 5340 paired images of six water types, out of which 4500 paired images are utilized for training, 500 paired for validation, and 340 for testing purposes.

## 5. Experiments and Results

This section describes the parameter settings in the proposed architecture and training approach, followed by the

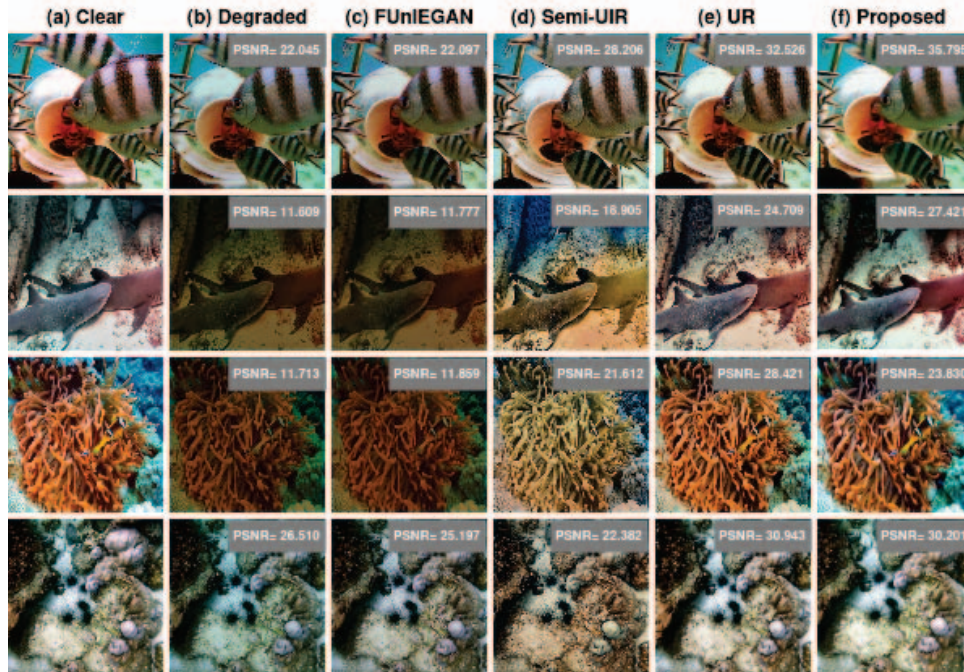


Figure 3: Visual analysis of the proposed method and PSNR values. column (a) contains the clear images, column (b) contains the degraded images in our dataset, column (c)-(e) contains the visual results of FUNIE-GAN[41], Semi-UIR [42], Underwater Ranker [43], (f) contains the visual results of our proposed method

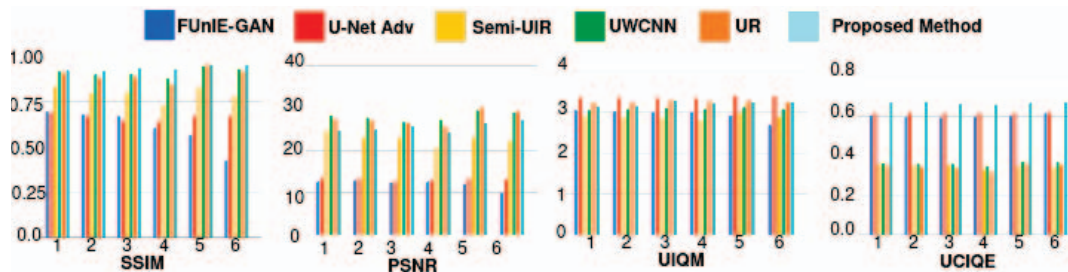


Figure 4: Ablation study is performed with different water types and five state-of-the-art methods: FUNIE-GAN[41], U-Net Adv [13], Semi-UIR [42], UWCNN [47], Underwater Ranker[43], and our proposed method

analysis of results in both qualitative and quantitative ways. The proposed method is tested against twenty-two state-of-the-art methods in terms of reference and no-reference underwater image quality metrics.

### 5.1. Parameter Setting and Training

The proposed method is trained on Intel(R) Core(TM) i5-10500 CPU, 3.10 GHz processor with 32GB RAM, and NVIDIA Quadro P1000 GPU. For the training process, the synthesized dataset images are resized to a fixed dimension of  $256 \times 256$ . The model is trained with a learning rate of 0.0001 and a batch size of 4 in the PyTorch framework. Our approach first focuses on training the encoder and decoder to reach a threshold of 0.9 to ensure that the encoder pro-

duces a latent vector  $Z$  that contains meaningful features. Upon achieving this, we introduce the water-type classifier ( $N$ ) and train it to a sufficient level so that it can guide the model towards adversarial learning of the encoder. The aim is to produce the latent vectors  $Z$  that are agnostic of the water type present and allow the model to produce an enhanced image that is independent of the water type.

### 5.2. Visual Analysis of the Results

The performance of the proposed scheme is verified with the regenerated data over UIEB for the visual analysis of the results. Figure 3 contains visual results on the proposed synthetic dataset on three state-of-the-art methods: FUNIE-GAN[41], Semi-UIR [42], Underwater Ranker [43] and our

Table 2: Quantitative result of Image Enhancement on UIEB dataset in terms of SSIM, PSNR, UIQM, UCIQE. Red denoted best and blue denotes second best

Methods	SSIM	PSNR	UIQM	UCIQE
IBLA[48]	0.805	17.925	1.383	0.586
ULAP [49]	0.745	15.855	1.427	0.597
SMBL [50]	0.801	16.681	1.319	0.593
UWGAN [51]	0.756	14.121	1.205	0.502
UWCNN [47]	0.65	13.177	1.202	0.469
FUnIE-GAN [41]	0.689	16.759	<b>2.894</b>	0.547
UColor [52]	0.873	21.888	1.187	0.556
MFEF [53]	<b>0.910</b>	<b>23.352</b>	1.333	<b>0.602</b>
UCM [54]	0.78	17.441	2.695	0.571
UDCP [55]	0.493	11.007	1.748	0.581
UGAN [56]	0.698	16.338	2.49	0.564
UAGAN [57]	0.773	18.093	2.957	0.599
Proposed	<b>0.936</b>	<b>25.581</b>	<b>3.214</b>	<b>0.666</b>

Table 3: Quantitative Result of Image Enhancement on EUVP dataset in terms of UIQM score. Red denotes best and Blue denotes second best.

Model	UIQM Score $\uparrow$	Std Deviation $\downarrow$
Res-WGAN[30]	2.46	0.67
Res-GAN[31]	2.62	0.89
LS-GAN[32]	2.59	0.52
Pix2Pix[58]	2.76	0.39
UGAN-P [33]	2.77	<b>0.34</b>
Cycle GAN[34]	2.62	0.67
FUnIE GAN[41]	<b>2.81</b>	0.65
Proposed	<b>3.18</b>	<b>0.22</b>

proposed method. It is clear from the figure that state-of-the-art methods fail to preserve the contrast of the image. The enhanced images produced by our proposed method look quite close to ground-truth images.

### 5.3. Quantitative Analysis of Results

The proposed method is evaluated quantitatively by using four metrics: Structural Similarity Index Measure (SSIM) [59], Peak Signal to Noise Ratio (PSNR) [60], Universal Image Quality Index (UIQM) [61], and Universal Color Image Quality Evaluator (UCIQE) [62].

Table 2 contains the quantitative analysis of the proposed scheme against twelve SOTA close competitive techniques: IBLA [48], ULAP [49], SMBL [50], UWGAN [51], UWCNN [47], FUnIE-GAN [41], Ucolor [52], MFEF [53], UCM [54], UDCP [55], UGAN [56], UAGAN [57] in terms of SSIM, PSNR, UIQM, and UCIQE with a test set of 340 images recreated on UIEB dataset. Our proposed model performed best compared to SOTA architectures in terms of SSIM, PSNR, UIQM, and UCIQE. Further, we evaluated the performance of our model on the EUVP dataset with seven state-of-the-art methods. Table 3 contains the result in terms of UIQM measure and standard deviation of the same. it may be concluded from the said table that, our pro-

posed architecture outperformed the state-of-the-art methods.

## 6. Ablation studies

An ablation study is performed to test the effectiveness of the proposed model in terms of loss functions used and the introduction of the water-type classifier. An ablation study is performed using various combinations of loss functions used in the proposed scheme and is shown in Table 4. R represents reconstruction loss, C is classifier loss, and A is the adversarial loss. Combining R, C, and A produces enhanced images while preserving details across various domains. Hence, the proposed method uses a combination of all three losses. Further, the test images from the proposed six water types are evaluated against five state-of-the-art methods, and results in terms of SSIM, PSNR, UIQM, and UCIQE are presented in Fig 4. The highest variance compared to water type is observed in structural similarity. Hence, a change in degradation level directly impacts the preservation of minute details in the image. It is clear that our proposed model preserves the minute details while generating visually appealing images and compensating for the underwater degradations.

Table 4: Ablation study is performed with combinations of different R, C, and A values. R stands for Reconstruction loss, C stands for classifier loss, and A stands for adversarial loss.

Losses $\rightarrow$	R	C	A	R	C	A	R	C	A
Metric $\downarrow$	$\checkmark$	$\checkmark$		$\checkmark$		$\checkmark$	$\checkmark$	$\checkmark$	$\checkmark$
SSIM		0.9103			<b>0.951</b>				<b>0.9359</b>
PSNR		21.224			<b>26.60</b>				<b>25.628</b>
UIQM		<b>3.3142</b>			3.209				<b>3.2157</b>
UCIQE		0.6556			<b>0.6650</b>				<b>0.6668</b>

## 7. Conclusion and Future Work

In this paper, we introduced a novel domain adversarial network to learn the features across different water types. The proposed architecture consists of the encoder-decoder network to remove the distortion from the degraded underwater images. Further, a classifier network is deployed to generalize over distribution among varied data types. A synthetic dataset of six classes is designed according to the different attenuation constants. We corroborated our findings against twenty-two SOTA architectures. Our proposed method gave a state-of-the-art performance in terms of reference and no-reference image quality assessment metrics. Further, our proposed model preserves the minute details without introducing any ghosts. In the future, we would like to test the model for low-light underwater environment conditions.



## References

- [1] D. K. Rout, B. N. Subudhi, T. Veerakumar, and S. Chaudhury, "Walsh-hadamard-kernel-based features in particle filter framework for underwater object tracking," *IEEE Transactions on Industrial Informatics*, vol. 16, no. 9, pp. 5712–5722, 2019.
- [2] J. Agbakwuru, "Oil/gas pipeline leak inspection and repair in underwater poor visibility conditions: challenges and perspectives," *Journal of Environmental Protection*, vol. 03, 01 2012.
- [3] P. A. Miller, J. A. Farrell, Y. Zhao, and V. Djapic, "Autonomous underwater vehicle navigation," *IEEE Journal of Oceanic Engineering*, vol. 35, no. 3, pp. 663–678, 2010.
- [4] C. Sanchez-Ferreira, H. Hultmann Ayala, L. Coelho, D. Muñoz, M. Farias, and C. Llanos, "Multi-objective differential evolution algorithm for underwater image restoration," in *IEEE Congress on Evolutionary Computation (CEC)*, pp. 243–250, 05 2015.
- [5] S. S. Agaian, B. Silver, and K. A. Panetta, "Transform coefficient histogram-based image enhancement algorithms using contrast entropy," *IEEE Transactions on Image Processing*, vol. 16, no. 3, pp. 741–758, 2007.
- [6] S. M. Pizer, E. P. Amburn, J. D. Austin, R. Cromartie, A. Geselowitz, T. Greer, B. ter Haar Romeny, J. B. Zimmerman, and K. Zuiderveld, "Adaptive histogram equalization and its variations," *Computer Vision, Graphics, and Image Processing*, vol. 39, no. 3, pp. 355–368, 1987.
- [7] W. Zhang, P. Zhuang, H.-H. Sun, G. Li, S. Kwong, and C. Li, "Underwater image enhancement via minimal color loss and locally adaptive contrast enhancement," *IEEE Transactions on Image Processing*, vol. 31, pp. 3997–4010, 2022.
- [8] R. Caballero and A. Berbey-Alvarez, "Underwater image enhancement using dark channel prior and image opacity," in *Proceedings of 7th International Engineering, Sciences and Technology Conference (IESTEC)*, pp. 556–561, 2019.
- [9] D. K. Rout, B. N. Subudhi, T. Veerakumar, S. Chaudhury, and J. Soraghan, "Multiresolution visual enhancement of hazy underwater scene," *Multimedia Tools and Applications*, vol. 81, no. 23, pp. 32 907–32 936, 2022.
- [10] P. Zhuang, J. Wu, F. Porikli, and C. Li, "Underwater image enhancement with hyper-laplacian reflectance priors," *IEEE Transactions on Image Processing*, vol. 31, pp. 5442–5455, 2022.
- [11] L. Chen, Z. Jiang, L. Tong, Z. Liu, A. Zhao, Q. Zhang, J. Dong, and H. Zhou, "Perceptual underwater image enhancement with deep learning and physical priors," *IEEE Transactions on Circuits and Systems for Video Technology*, vol. 31, no. 8, pp. 3078–3092, 2021.
- [12] R. Liu, Z. Jiang, S. Yang, and X. Fan, "Twin adversarial contrastive learning for underwater image enhancement and beyond," *IEEE Transactions on Image Processing*, vol. 31, pp. 4922–4936, 2022.
- [13] P. M. Uplavikar, Z. Wu, and Z. Wang, "All-in-one underwater image enhancement using domain-adversarial learning," in *CVPR workshops*, pp. 1–8, 2019.
- [14] C. Li, C. Guo, W. Ren, R. Cong, J. Hou, S. Kwong, and D. Tao, "An underwater image enhancement benchmark dataset and beyond," *IEEE Transactions on Image Processing*, vol. 29, pp. 4376–4389, 2020.
- [15] V. Voronin, E. Semenishchev, S. Tokareva, A. Zelenskiy, and S. Agaian, "Underwater image enhancement algorithm based on logarithmic transform histogram matching with spatial equalization," in *2018 14th IEEE International Conference on Signal Processing (ICSP)*, pp. 434–438, 2018.
- [16] J. Ma, X. Fan, S. X. Yang, X. Zhang, and X. Zhu, "Contrast limited adaptive histogram equalization-based fusion in yiq and hsi color spaces for underwater image enhancement," *International Journal of Pattern Recognition and Artificial Intelligence*, vol. 32, no. 07, p. 1854018, 2018.
- [17] L. Bai, W. Zhang, X. Pan, and C. Zhao, "Underwater image enhancement based on global and local equalization of histogram and dual-image multi-scale fusion," *IEEE Access*, vol. 8, pp. 128 973–128 990, 2020.
- [18] H.-Y. Yang, P.-Y. Chen, C.-C. Huang, Y.-Z. Zhuang, and Y.-H. Shiau, "Low complexity underwater image enhancement based on dark channel prior," in *2011 Second International Conference on Innovations in Bio-inspired Computing and Applications*, pp. 17–20, 2011.
- [19] Z. Liang, X. Ding, Y. Wang, X. Yan, and X. Fu, "Gudcp: Generalization of underwater dark channel prior for underwater image restoration," *IEEE Transactions on Circuits and Systems for Video Technology*, vol. 32, no. 7, pp. 4879–4884, 2021.
- [20] R. Sathya, M. Bharathi, and G. Dhivyasri, "Underwater image enhancement by dark channel prior," in *2015 2nd International Conference on Electronics and Communication Systems (ICECS)*, pp. 1119–1123, 2015.
- [21] J. Zhou, D. Liu, X. Xie, and W. Zhang, "Underwater image restoration by red channel compensation and underwater median dark channel prior," *Applied Optics*, vol. 61, no. 10, pp. 2915–2922, 2022.
- [22] C.-Y. Cheng, C.-C. Sung, and H.-H. Chang, "Underwater image restoration by red-dark channel prior and point spread function deconvolution," in *2015 IEEE international conference on signal and image processing applications (ICSIPA)*, pp. 110–115, 2015.
- [23] Z. Sun, F. Li, W. Chen, and M. Wu, "Underwater image processing method based on red channel prior and retinex algorithm," *Optical Engineering*, vol. 60, no. 9, pp. 093 102–093 102, 2021.
- [24] S. Borkar and S. Bonde, "Underwater image restoration using single color channel prior," in *2016 International Conference on Signal and Information Processing (IconSIP)*, pp. 1–4, 2016.
- [25] M.-H. Cheng, T.-Z. Huang, X.-L. Zhao, T.-H. Ma, and J. Huang, "A variational model with hybrid hyper-laplacian priors for retinex," *Applied Mathematical Modelling*, vol. 66, pp. 305–321, 2019.

- [26] K. Jon, Y. Sun, Q. Li, J. Liu, X. Wang, and W. Zhu, "Image restoration using overlapping group sparsity on hyper-laplacian prior of image gradient," *Neurocomputing*, vol. 420, pp. 57–69, 2021.
- [27] Y. Wang, J. Guo, H. Gao, and H. Yue, "UIEC2-net: CNN-based underwater image enhancement using two color space," *Signal Processing: Image Communication*, vol. 96, p. 116250, 2021.
- [28] F. Han, J. Yao, H. Zhu, and C. Wang, "Underwater image processing and object detection based on deep CNN method," *Journal of Sensors*, vol. 2020, 2020.
- [29] Y. Wang, J. Zhang, Y. Cao, and Z. Wang, "A deep CNN method for underwater image enhancement," in *2017 IEEE international conference on image processing (ICIP)*, pp. 1382–1386, 2017.
- [30] M. Arjovsky, S. Chintala, and L. Bottou, "Wasserstein generative adversarial networks," in *Proceedings of the 34th International Conference on Machine Learning*, ser. Proceedings of Machine Learning Research, vol. 70, pp. 214–223, 08 2017.
- [31] J. Li, X. Liang, Y. Wei, T. Xu, J. Feng, and S. Yan, "Perceptual generative adversarial networks for small object detection," *Proceedings of the IEEE conference on computer vision and pattern recognition*, pp. 1222–1230, 2017.
- [32] X. Mao, Q. Li, H. Xie, R. Y. K. Lau, and Z. Wang, "Multi-class generative adversarial networks with the L2 loss function," *CoRR: a computing research repository*, vol. 5, pp. 1057–7149, 2016.
- [33] C. Fabbri, M. J. Islam, and J. Sattar, "Enhancing underwater imagery using generative adversarial networks," *IEEE International Conference on Robotics and Automation (ICRA)*, pp. 7159–7165, 2018.
- [34] J.-Y. Zhu, T. Park, P. Isola, and A. A. Efros, "Unpaired image-to-image translation using cycle-consistent adversarial networks," in *Proceedings of IEEE International Conference on Computer Vision (ICCV)*, pp. 2242–2251, 2017.
- [35] I. Goodfellow, J. Pouget-Abadie, M. Mirza, B. Xu, D. Warde-Farley, S. Ozair, A. Courville, and Y. Bengio, "Generative adversarial networks," *Communications of the ACM*, vol. 63, no. 11, pp. 139–144, 2020.
- [36] P. Isola, J.-Y. Zhu, T. Zhou, and A. A. Efros, "Image-to-image translation with conditional adversarial networks," in *Proceedings of IEEE Conference on Computer Vision and Pattern Recognition (CVPR)*, pp. 5967–5976, 2017.
- [37] Y. Guo, H. Li, and P. Zhuang, "Underwater image enhancement using a multiscale dense generative adversarial network," *IEEE Journal of Oceanic Engineering*, vol. PP, pp. 1–9, 06 2019.
- [38] A. Ignatov, N. Kobyshev, R. Timofte, K. Vanhoey, and L. Van Gool, "DSLR-quality photos on mobile devices with deep convolutional networks," in *Proceedings of the IEEE international conference on computer vision*, pp. 3277–3285, 2017.
- [39] J. Johnson, A. Alahi, and L. Fei-Fei, "Perceptual losses for real-time style transfer and super-resolution," in *Proceeding of 14th European Conference, Amsterdam*.
- [40] T.-Y. Lin, P. Goyal, R. Girshick, K. He, and P. Dollár, "Focal loss for dense object detection," in *Proceedings of the IEEE international conference on computer vision*, pp. 2980–2988, 2017.
- [41] M. J. Islam, Y. Xia, and J. Sattar, "Fast underwater image enhancement for improved visual perception," *IEEE Robotics and Automation Letters*, vol. 5, no. 2, pp. 3227–3234, 2020.
- [42] S. Huang, K. Wang, H. Liu, J. Chen, and Y. Li, "Contrastive semi-supervised learning for underwater image restoration via reliable bank," in *Proceedings of the IEEE/CVF Conference on Computer Vision and Pattern Recognition*, pp. 18 145–18 155, 2023.
- [43] C. Guo, R. Wu, X. Jin, L. Han, W. Zhang, Z. Chai, and C. Li, "Underwater ranker: Learn which is better and how to be better," in *Proceedings of the AAAI Conference on Artificial Intelligence*, vol. 37, no. 1, pp. 702–709, 2023.
- [44] M. G. Solonenko and C. D. Mobley, "Inherent optical properties of jerlov water types," *Applied optics*, vol. 54, no. 17, pp. 5392–5401, 2015.
- [45] D. Akkaynak, T. Treibitz, T. Shlesinger, Y. Loya, R. Tamir, and D. Iluz, "What is the space of attenuation coefficients in underwater computer vision?" in *Proceedings of the IEEE Conference on Computer Vision and Pattern Recognition*, pp. 4931–4940, 2017.
- [46] N. G. Jerlov, "Marine optics," in *Energy Security and Global Politics: The Militarization of Resource Management*, ser. Elsevier Oceanography Series, N. Jerlov, Ed. New York, NY, USA: Elsevier, 1976, pp. 130–135.
- [47] C. Li, S. Anwar, and F. Porikli, "Underwater scene prior inspired deep underwater image and video enhancement," *Pattern Recognition*, vol. 98, p. 107038, 2020.
- [48] Y.-T. Peng and P. C. Cosman, "Underwater image restoration based on image blurriness and light absorption," *IEEE transactions on image processing*, vol. 26, no. 4, pp. 1579–1594, 2017.
- [49] W. Song, Y. Wang, D. Huang, and D. Tjondronegoro, "A rapid scene depth estimation model based on underwater light attenuation prior for underwater image restoration," in *Advances in Multimedia Information Processing–PCM 2018: 19th Pacific-Rim Conference on Multimedia, Hefei, China, September 21-22, 2018, Proceedings, Part I 19*, pp. 678–688, 2018.
- [50] W. Song, Y. Wang, D. Huang, A. Liotta, and C. Perra, "Enhancement of underwater images with statistical model of background light and optimization of transmission map," *IEEE Transactions on Broadcasting*, vol. 66, no. 1, pp. 153–169, 2020.
- [51] N. Wang, Y. Zhou, F. Han, H. Zhu, and J. Yao, "Uwgan: underwater gan for real-world underwater color restoration and dehazing," *arXiv preprint arXiv:1912.10269*, 2019.

- [52] C. Li, S. Anwar, J. Hou, R. Cong, C. Guo, and W. Ren, "Underwater image enhancement via medium transmission-guided multi-color space embedding," *IEEE Transactions on Image Processing*, vol. 30, pp. 4985–5000, 2021.
- [53] J. Zhou, J. Sun, W. Zhang, and Z. Lin, "Multi-view underwater image enhancement method via embedded fusion mechanism," *Engineering Applications of Artificial Intelligence*, vol. 121, p. 105946, 2023.
- [54] K. Iqbal, M. Odetayo, A. James, R. A. Salam, and A. Z. H. Talib, "Enhancing the low quality images using unsupervised colour correction method," in *2010 IEEE International Conference on Systems, Man and Cybernetics*, pp. 1703–1709, 2010.
- [55] P. L. Drews, E. R. Nascimento, S. S. Botelho, and M. F. M. Campos, "Underwater depth estimation and image restoration based on single images," *IEEE computer graphics and applications*, vol. 36, no. 2, pp. 24–35, 2016.
- [56] C. Fabbri, M. J. Islam, and J. Sattar, "Enhancing underwater imagery using generative adversarial networks," in *2018 IEEE international conference on robotics and automation (ICRA)*, pp. 7159–7165, 2018.
- [57] N. Wang, T. Chen, X. Kong, Y. Chen, R. Wang, Y. Gong, and S. Song, "Underwater attentional generative adversarial networks for image enhancement," *IEEE Transactions on Human-Machine Systems*, 2023.
- [58] P. Isola, J.-Y. Zhu, T. Zhou, and A. A. Efros, "Image-to-image translation with conditional adversarial networks," in *Proceedings of IEEE Conference on Computer Vision and Pattern Recognition (CVPR)*, pp. 5967–5976, 2017.
- [59] Z. Wang, A. Bovik, H. Sheikh, and E. Simoncelli, "Image quality assessment: from error visibility to structural similarity," *IEEE Transactions on Image Processing*, vol. 13, no. 4, pp. 600–612, 2004.
- [60] M. Pieraccini, N. Rojhani, and L. Miccinesi, "MIMO radar with dense or random pattern: Analysis of phase and positioning error sensitivity," in *2019 Photonics & Electromagnetics Research Symposium-Spring (PIERS-Spring)*, pp. 1098–1105, 06 2019.
- [61] K. Panetta, C. Gao, and S. Agaian, "Human-visual-system-inspired underwater image quality measures," *IEEE Journal of Oceanic Engineering*, vol. 41, no. 3, pp. 541–551, 2016.
- [62] M. Yang and A. Sowmya, "An underwater color image quality evaluation metric," *IEEE Transactions on Image Processing*, vol. 24, no. 12, pp. 6062–6071, 2015.